# Ectopic Activity of Fibroblast Growth Factor Receptor 1 in Hepatocytes Accelerates Hepatocarcinogenesis by Driving Proliferation and Vascular Endothelial Growth Factor–Induced Angiogenesis

**Xinqiang Huang, Chundong Yu, Chengliu Jin, Masashi Kobayashi, Courtney A. Bowles, Fen Wang, and Wallace L. McKeehan**

Center for Cancer Biology and Nutrition, Institute of Biosciences and Technology, Texas A&M University System Health Science Center, Houston, Texas

## Abstract

**Fibroblast growth factor (FGF) signaling mediates cell-to-cell communication in development and organ homeostasis in adults. Of the four FGF receptor (FGFR) tyrosine kinases, only FGFR4 is expressed in mature hepatocytes. Although FGFR1 is expressed by hepatic cell progenitors and adult nonparenchymal cells, ectopic expression is commonly observed in hepatoma cells. Here, we determined whether ectopic FGFR1 is a cause or consequence of hepatocellular carcinoma by targeting a constitutively active human FGFR1 to mouse hepatocytes. Livers of transgenic mice exhibited accelerated regeneration after partial hepatectomy but no signs of neoplastic or preneoplastic abnormalities for up to 18 months. However, in diethylnitrosamine-treated mice, the chronic FGFR1 activity promoted an incidence of 44% adenomas at 4 months and 38% hepatocellular carcinoma at 8 months. No adenoma or hepatocellular carcinoma was observed in diethylnitrosamine-treated wild-type (WT) livers at 4 or 8 months, respectively. At 10 and 12 months, tumor-bearing livers in transgenic mice were twice the size of those in WT animals. Isolated hepatoma cells from the transgenic tumors exhibited a growth advantage in culture. Advanced hepatocellular carcinoma in the transgenic livers exhibited a reduced rate of necrosis. This was accompanied by a mean microvessel density of 2.7 times that of WT tumors and a markedly higher level of vascular endothelial growth factor. In cooperation with an initiator, the persistent activity of ectopic FGFR1 in hepatocytes is a strong promoter of hepatocellular carcinoma by driving cell proliferation at early stages and promoting neoangiogenesis at late stages of progression.** (Cancer Res 2006; 66(3): 1481-90)

## Introduction

Hepatocellular carcinoma, the most common primary liver cancer, ranks fifth in frequency worldwide with an estimated 0.5 million new cases every year. It is the third leading cause of cancer deaths (1, 2). Constitutive expression or losses of polypeptide regulators and their receptors that promote or control cell growth, respectively, are associated with hepatocellular carcinoma (3–7). The presence, compartmentation, activity, and changes in members of the fibroblast growth factor (FGF) family implicate FGF signaling in both liver development and homeostasis in adults (8, 9). FGFs from cardiac mesoderm cause development of liver from foregut endoderm where FGF receptor (FGFR) 1 and 4 are expressed (10). Ablation of both FGF1 and FGF2 in mice indicates that neither plays a direct role in hepatocyte proliferation. However, both contribute to matrix deposition and hepatolobular restoration in the adult in response to injury (11). Although mRNA levels are very low, resting adult livers contain abundant reserves of FGF1 and FGF2 protein at levels higher than most other tissues (12). FGF1 and FGF2 mRNAs increase in response to partial hepatectomy or damage (13–15). Other FGF homologues have been reported in liver, but their significance, cellular target, and physiologic role are unclear (16). The mRNAs of all four FGFR tyrosine kinase mRNAs have been reported in adult liver (17–19). Expression of FGFR1 and FGFR4 are strictly compartmented. FGFR4 is exclusively expressed in the hepatocytes, whereas FGFR1 is limited to nonparenchymal cells (17, 20). Studies using FGFR4 knockout mice revealed that hepatocyte FGFR4 plays roles in maintenance of liver functional homeostasis rather than a direct role in compensatory hepatocyte proliferation. FGFR4 signaling interfaces with metabolite-controlled transcription networks to regulate cholesterol to bile acid synthesis (21, 22). In addition, FGFR4 plays a role in limitation of internal liver injury by toxic products of liver metabolism (23).

Ectopic or chronic expression of specific FGF and FGFR isotypes is commonly observed in tumors (8, 9, 24, 25). Aberrant expression of isotypes other than resident hepatocyte FGFR4 has been observed in human hepatoma cell lines, clinical tissues, and animal models (26–28). Expression of FGFR1 mRNA is elevated in livers bearing hepatocellular carcinoma and so are their activators FGF1 and FGF2 (27, 28). In contrast to normal hepatocytes (20), hepatoma cell lines in culture commonly express FGFR1 (26, 28). It is unclear whether elevated expression of FGFR1 actively contributes to development of hepatocellular carcinoma or is merely a consequence of aberrant gene expression in the tumor. To clarify this, we forced ectopic and chronic expression of FGFR1 in hepatocytes by targeting an albumin promoter-driven cDNA coding for a constitutively active human FGFR1 (caFGFR1) to mouse liver. Ectopic expression of caFGFR1 in hepatocytes increased the number of proliferating hepatocytes in response to

**Note:** C. Yu is currently at the Department of Molecular and Cellular Biology, Baylor College of Medicine, One Baylor Plaza, Houston, TX 77030. M. Kobayashi is currently at the Department of Molecular Oral Medicine and Maxillofacial Surgery, Division of Frontier Medical Science, Graduate School of Biomedical Sciences, Hiroshima University, Hiroshima, Japan.

**Requests for reprints:** Wallace L. McKeehan, Center for Cancer Biology and Nutrition, Institute of Biosciences and Technology, Texas A&M University System Health Science Center, 2121 West Holcombe Boulevard, Houston, TX 77030. Phone: 713-677-7522; Fax: 713-677-7512; E-mail: wmckeehan@ibt.tamhsc.edu.



doi:10.1158/0008-5472.CAN-05-2412

partial hepatectomy but failed to induce preneoplasia or neoplasia. Although incapable of initiation of hepatomas on its own, we showed that the ectopic expression and chronic activity of FGFR1 was a strong promoter of diethylnitrosamine-initiated hepatocarcinogenesis both as a proliferative enhancer and as a promoter of neoangiogenesis mediated by vascular endothelial growth factor (VEGF).

## Materials and Methods

**Transgenic mice.** The construction of FLAG-caFGFR1 cDNA was described previously (29). The FLAG sequence was inserted into the $NH_2$ terminus of human FGFR1 at a site confirmed to have no effect on FGFR1 activity (29). The cDNA was inserted downstream of a hepatocyte-specific 2.3-kb albumin promoter (a gift from Dr. S. Thorgeirsson, NIH, Bethesda, MD) in SK-ALB/SV40 T vector (30). A chicken insulator was inserted at the 3′ end of the transgene at a *Xba*I site. The ALB-FLAG-caFGFR1 gene was excised by treatment with *Bss*HII, purified, and employed to produce transgenic FVB mice by pronuclear injection and implantation. Transgenic mice were identified by Southern hybridization of *Eco*RI-digested tail genomic DNA with $^{32}$P-labeled FGFR1 cDNA or by PCR as described previously (29). Transgenic and wild-type (WT) mice were produced by mating heterozygous caFGFR1 transgenic males with WT FVB females. Due to a higher incidence of diethylnitrosamine-induced hepatocellular carcinoma in males, the study was limited to male mice. All mouse work was done in accordance with the Institutional Animal Care and Use Committee at the Institute of Biosciences and Technology, Texas A&M University System Health Science Center. Bile acids were measured in both transgenic and WT mice as described previously (21).

**Partial hepatectomy, liver regeneration, and DNA synthesis.** Liver regeneration induced by partial hepatectomy and subsequent analysis was done as described previously (21). Briefly, one third of the liver was surgically removed from three to four transgenic and WT male mice at 2 to 3 months of age. Mice were sacrificed and analyzed at the times indicated in the text. DNA synthesis was monitored by i.p. administration of 50 μg bromodeoxyuridine (BrdUrd)/g body weight. BrdUrd-positive cells in paraffin sections were detected with anti-BrdUrd monoclonal antibody (Sigma, St. Louis, MO). Positively stained cells in four to five fields at ×200 magnification per tissue section for three different sections from each mouse were counted manually. The incidence of BrdUrd incorporation was expressed as the percentage of positive staining hepatocyte nuclei.

**Analysis of livers from diethylnitrosamine-treated mice.** Cohorts of transgenic mice and WT littermates were subjected to a single i.p. injection of 10 μg/g body weight of diethylnitrosamine (Sigma) 15 days after birth. Mice were sacrificed at 4, 6, 8, 10, and 12 months after birth. Whole body weights were recorded and the livers were excised, weighed, and examined for macroscopic lesions. Large macroscopic lesions were dissected out or when there was no visible tumor ~0.2 $cm^3$ of tissue from the same position on each lobe of the liver was sampled. Tissue was fixed overnight in Histochoice Tissue Fixative MB (Amresco, Solon, OH) or in 10% neutral buffered formalin (Richard-Allan Scientific, Kalamazoo, MI), dehydrated through a series of ethanol treatments, embedded in paraffin, sectioned serially at 5 μm, and stained with H&E for histopathologic analysis according to standard methods. Three sections that were at least 300 μm apart were analyzed from each tissue. A portion of each tissue or tumor was archived by quick freezing in liquid nitrogen and stored at −80°C.

DNA synthesis in diethylnitrosamine-treated livers was assessed as described above for partial hepatectomy.

**Terminal deoxynucleotidyl transferase–mediated dUTP nick end labeling assay for apoptotic cells.** Cells in apoptosis were assessed by the *in situ* terminal deoxynucleotidyl transferase–mediated dUTP nick end labeling (TUNEL) method according to the manufacturer's instructions using an *In situ* Cell Death Detection kit (Promega, Madison, WI). Sections were counterstained with propidium iodide. Positive cells were counted and the apoptosis index was expressed as the number of labeled hepatocytes per 1,000 cells counted in four to five fields at ×300 magnification.

**Analysis of mRNA expression.** Total RNA was isolated from liver with Ultraspec RNA Isolation System (Biotecx Laboratories, Houston, TX). Specific mRNAs were measured by RNase protection assay (RPA) using the HybSpeed RPA kit (Ambion, Austin, TX). For RPA, liver RNA (~40 μg) was hybridized with $1 \times 10^5$ counts/min $^{32}$P-labeled specific and β-actin antisense riboprobes in the same reaction mixture. After treatment with RNase, protected products were analyzed on 5% polyacrylamide sequencing gels followed by autoradiography. Reverse transcription was carried out with SuperScript II (Life Technologies, Grand Island, NY) and random primers according to protocols provided by the manufacturer. The PCR was carried out for 40 cycles at 94°C for 1 minute, 55°C or 60°C for 1 minute, and 72°C for 1 minute using Taq DNA polymerase (Promega) and specific primers. Murine FGFR1 was amplified by reverse transcription-PCR (RT-PCR) from mouse liver using sense primer 5′-ATACGTGTTGGCGGGTAACTC and antisense primer 5′-TGCACAGCCATCTGGCTATGGA. Murine VEGF was amplified by RT-PCR from mouse liver using sense primer 5′-TGTACCTCCACCATGCCAAGTG and antisense primer 5′-ATCGTTACAGCAGCCTGCACAG. Murine β-actin cDNA was described previously (21). The products of RT-PCR were verified by sequencing. Riboprobes complementary to part of the cDNAs described above, which have been subcloned into pBluescript-SK, were transcribed into $^{32}$P-labeled antisense riboprobes by T3 or T7 RNA polymerase using the MAXiscript kit (Ambion). The size of probes and the predicted protected fragments were as follows: human FGFR1, 310 and 282 nucleotides; murine FGFR1, 315 and 239 nucleotides; murine VEGF, 294 and 218 nucleotides; and β-actin, 197 and 139 nucleotides.

**Immunochemical analyses.** Unless otherwise noted, all procedures were carried out at 4°C. Frozen liver tissues were homogenized in radioimmunoprecipitation assay buffer (1× PBS, 1% NP40, 0.5% sodium deoxycholate, 0.1% SDS). After standing for 30 minutes on ice, homogenates were clarified by centrifugation. Protein concentrations were determined using the BCA Protein Assay Reagent (Pierce, Rockford, IL). For immunoprecipitation, 1 mL liver lysate supernatants containing 1 mg protein was incubated with 4 μg anti-FLAG M2 monoclonal antibody for 2 hours. Immune complexes were captured overnight by addition of 20 μL protein G-Sepharose followed by centrifugation at 2,500 rpm for 30 seconds and washing thrice with PBS. For Western blot analysis, immunoprecipitates or 30 μg isolated hepatoma cell lysate (described below) was applied to 8% SDS-PAGE, transferred to Hybond-P membrane (Amersham, Piscataway, NJ), which was incubated with the primary antibody, washed thrice, and then incubated with the second anti-mouse or anti-rabbit IgG conjugated to horseradish peroxidase (Bio-Rad, Hercules, CA). Bands were visualized by development with the Enhanced Chemiluminescence Plus detection reagents (Amersham). Primary antibodies indicated in the text and used for Western blots were rabbit anti-human FGFR1 antiserum (Santa Cruz Biotechnology, Santa Cruz, CA), mouse anti-FLAG M2 antibody (Sigma), and mouse anti-phosphorylated mitogen-activated protein kinase [MAPK; extracellular signal-regulated kinase (ERK) 1/2; Upstate, Lake Placid, NY]. Immunohistochemical analysis was done on 5-μm paraffin sections mounted on Superfrost/Plus slides (Fisher Scientific, Pittsburgh, PA). After antigen retrieval by 0.01% trypsin, sections were then incubated with VEGF polyclonal antibody (1:50, Santa Cruz Biotechnology) or an anti-human von Willebrand factor (vWf) rabbit antibody (1:50, DAKO Corp., Carpinteria, CA) overnight. For the BrdUrd analyses, sections were further incubated in 0.2 N HCl at 37°C for 30 minutes before application of the BrdUrd monoclonal antibody (1:500). Primary antibodies were detected using the ExtrAvidin Peroxidase Staining kit (Sigma) according to the manufacturer's instructions.

**Evaluation of microvessel density.** The microvessel density (MVD) within hepatocellular carcinoma was evaluated by immunostaining with vWf antibody. Tumor sections were first screened at low power (×40) to identify areas of highest MVD. Counting was done in the three highest areas of MVD observed at high power (×200). Positively stained endothelial cells or endothelial cell clusters that were clearly separate from an adjacent microvessel or tumor cells were scored as one microvessel independent of presence of an intact vessel lumen. The mean value of counts from three fields was considered representative of the MVD of an individual tumor.

**Hepatoma cell culture.** Surface tumors were excised from transgenic and WT mice, washed in PBS solution with 100 units/mL kanamycin, and minced into small pieces. The minced tissue was further dissociated into cell aggregates and single cells by treatment with 0.14 units/mL liberase RH (Roche, Indianapolis, IN) in RD medium (1:1 RPMI and DMEM) for 30 to 60 minutes at 37°C. The dissociated tissue suspension was filtered through 12-ply gauze pads to remove large cell aggregates and the filtrate containing ~75% single cells was suspended in RD medium with 10% fetal bovine serum (FBS). Aliquots of cell suspensions containing $\sim 1.0 \times 10^6$ cells were then inoculated into 25-$cm^2$ cell culture flasks (Corning, Inc., Corning, NY) in 4 mL medium and incubated in 5% $CO_2$ at 37°C. Cell attachment was maximal after 2 hours, and the medium was discarded, replaced, and changed every 5 days thereafter. Cultures were observed every 2 to 3 days. Over a 1- to 2-week period, islands of cells with hepatocyte-like morphology appeared that continued to slowly expand. When cells occupied ~30% of the surface area, cells were harvested by exposure to 75 mg/L Pronase and 0.02% EDTA for 10 minutes at 37°C, placed in new flasks and media, and grown to confluent monolayers. Confluent monolayers were harvested and new cultures were thereafter established by seeding $\sim 2 \times 10^5$ cells into flasks containing 3 mL culture medium. The cell population was continuously cultured by the same procedures over a period of 3 months until apparently stable with respect to rate of expansion to confluency at which time they were used in cell proliferation and functional assays. Stock cultures were banked at every fifth passage.

DNA synthesis was determined by measuring the rate of incorporation of [$^3$H]thymidine into DNA. Cells were plated in 24-well plates at a density of $3 \times 10^4$ per well in 0.5 mL RD medium containing 10% FBS overnight. Attached cells were exposed to serum-free RD medium for 24 hours. Cells were further incubated for an additional 24 hours in serum-free medium, serum-free medium containing 20 ng/mL FGF1, or 10% FBS-containing medium. For the last 6 hours of incubation, 0.25 μCi/well [$^3$H]thymidine was added. Cells were then washed with PBS, fixed in cold 10% trichloroacetic acid, and lysed in 0.4 N NaOH. Thymidine incorporation was determined using a scintillation counter. For cell proliferation determinations, $3 \times 10^3$ cells were seeded into 96-well plates in 100 μL RD medium containing 10% FBS. The next day, the medium was changed to the 10% FBS-containing medium or replaced with medium containing 0.5% FBS (day 0) and incubated for the times indicated in the text. Cell numbers within a population were estimated with Cell Proliferation Kit I [3-(4,5-dimethylthiazol-2-yl)-2,5-diphenyltetrazolium bromide; Roche] according to the manufacturer's suggestions. Data from plates were collected using a VERSAmax microplate reader at 570 nm. Three independent experiments of four wells were done for each variable with two independent cell lines.

**Statistical analysis.** Values were expressed as mean ± SD from the numbers of replicates described in the figure legends. Statistical significance was determined by Student's $t$ test with a significance threshold of $P < 0.05$.

## Results

**Ectopic expression of caFGFR1 in hepatocytes.** To determine whether the persistent inappropriate expression of FGFR1 in hepatocytes could initiate and promote hepatocellular carcinoma, we targeted ectopic human FGFR1 to specifically the mature hepatocytes in FVB mice using the albumin promoter. To bypass the need for the constant presence of a FGF activator, a ligand-independent, constitutively active mutant (caFGFR1) with a single amino acid substitution of glutamate for lysine in the kinase control domain was employed (ref. 29; Fig. 1*A*). Three of five transgenic identified by Southern blot hybridization or PCR analysis founders were used to establish transgenic lines. Expression of the transgene was first assessed with a RT-PCR screen using total liver mRNA (data not shown) and then quantitated by RPA using a human FGFR1 cRNA probe. RPA analysis indicated that caFGFR1 mRNA was significantly above the trace levels indicated by RT-PCR (Fig. 1*B*). The presence of the FLAG-tagged caFGFR1 transgene product was confirmed by double-antibody immunoprecipitation and immunoblot analysis of liver extracts (Fig. 1*C*). One line (designated line 11) with the highest apparent level of expression of caFGFR1 was chosen for characterization of phenotype. Over 50 transgenic mice were subjected to a complete autopsy and the livers were examined every 3 months up to 18 months. No overt difference in morphology, cellularity in either parenchymal or nonparenchymal compartments, proliferative activity monitored by incorporation of BrdUrd, or apoptotic activity was observed compared with WT littermates.

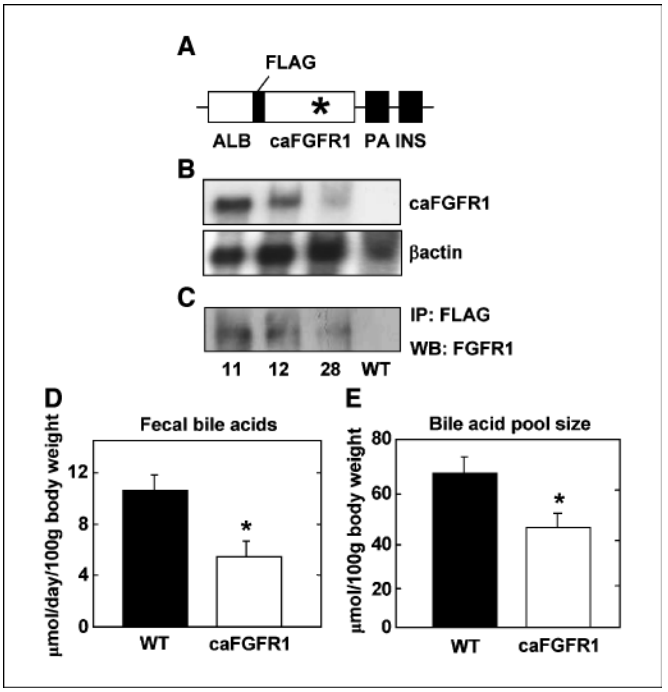


**Figure 1.** Targeting hyperactive FGFR1 to mouse hepatocytes. *A,* schematic of the caFGFR1 transgene. *ALB,* 2.3-kb albumin promoter; *FLAG,* coding sequence for the FLAG epitope (MDYKDDDDK); *caFGFR1,* coding sequence for human caFGFR1 (*asterisk,* a substitution of glutamate for lysine at position 656 that confers constitutive activity); *PA,* polyadenylate addition site for SV40 T antigens; *INS,* insulator. *B,* expression of the human caFGFR1 transgene mRNA. mRNA was determined by RPA as described in Materials and Methods. *C,* expression of caFGFR1 protein. Liver tissue extracts were subjected to immunoprecipitation with anti-FLAG antibody (*IP*) and the immunoprecipitate was analyzed by Western blot (*WB*) with anti-FGFR1 as described in Materials and Methods. Livers from three separate transgenic lines and WT were analyzed. *D,* fecal bile acid excretion. *E,* total bile acid pool. Bile acids were assessed as described (21). *Columns,* mean of 2-month-old mice (WT, $n = 5$ mice; caFGFR1, $n = 4$ mice); *bars,* SD. *, $P < 0.005$.

To ensure that the ectopic caFGFR1 was sufficiently active to cause a phenotype, we examined effect on cholesterol to bile acid metabolism. Mice lacking FGFR4 exhibit elevated bile acid synthesis (21), whereas mice expressing caFGFR4 exhibit depressed levels of synthesis (31). The results indicate that, similar to FGFR4, the expression of caFGFR1 in liver caused the fecal bile acids to decrease from 10.3 to 5.3 μmol/d/100 g body weight ($P < 0.005$; Fig. 1*D*) and the bile acid pool to decrease from 66 to 42 μmol/100 g body weight ($P < 0.005$; Fig. 1*E*). This indicated that ectopic FGFR1 in the hepatocyte has a similar effect on bile acid synthesis to resident hepatocyte FGFR4. This verified that transgenic levels of caFGFR1 were sufficiently active to cause a liver phenotype, although no overt changes associated with hyperplasia, preneoplasia, or neoplasia were apparent.

**Ectopic caFGFR1 accelerates rate of hepatocyte DNA synthesis after partial hepatectomy.** To determine whether ectopic hepatocyte FGFR1 contributed to compensatory growth of normal liver, DNA synthesis was monitored by immunohistochemical staining of BrdUrd incorporation in transgenic mice subjected to partial hepatectomy (Fig. 2*A*). At 48 hours after surgery, the average number of BrdUrd-positive hepatocyte nuclei was about twice higher ($P < 0.01$) in the caFGFR1 mice at the peak of DNA synthesis (Fig. 2*B*). This showed that FGFR1 is strongly mitogenic in hepatocytes when restraints on hepatocyte proliferation in normal resting liver have been removed.

**Chronic activity of ectopic FGFR1 in hepatocytes is a strong promoter of diethylnitrosamine-induced hepatocarcinogenesis.** Because the FGFR1 activity in hepatocytes caused no abnormalities associated with onset of neoplasia, we examined its potential promotion of hepatocellular carcinoma in cooperation with the strong initiator of liver carcinogenesis, diethylnitrosamine. Mice were subjected to a single exposure of 10 μg diethylnitrosamine/g body weight at 15 days of age. Livers of both transgenic and WT mice were examined at 4, 6, 8, 10, and 12 months. Visible surface tumor nodules appeared in caFGFR1 mice at 4 months (Fig. 3*A*; Table 1). In addition to a lack of surface nodules, no evidence of tumors were observed in WT controls treated with diethylnitrosamine after serial sectioning and examination for abnormalities. Examination of serial sections from nodules excised from the caFGFR1 livers at 4 months revealed that they were primarily composed of foci of typical hepatocellular adenomas that caused compression but no disruption of the surrounding normal tissue (Fig. 3*C* and *D*). At 6 months, some adenomas in the caFGFR1 mice were characterized by inclusion of fat droplets indicative of fatty liver and disruption of metabolism (Fig. 3*E*). Adenomas appeared in the diethylnitrosamine-treated WT controls at a frequency of 22% and 56%, respectively, at 6 to 8 months, but no hepatocellular carcinoma was apparent (Table 1). In the same period, total tumor incidence and size in the caFGFR1 mice significantly exceeded the WT controls. Lesions characteristic of hepatocellular carcinoma were apparent in 10% and 38% of the 6- and 8-month-old transgenic livers, respectively (Fig. 3*F* and *G*). Of the 1 in 10 of the 6-month-old caFGFR1 mice that exhibited hepatocellular carcinoma lesions, multiple foci of invasive hepatocellular carcinoma lesions were noted (Fig. 3*F*). Although they continued to increase, the hepatocellular carcinoma lesions in the ≥8-month caFGFR1 livers retained the typical trabecular hepatocellular carcinoma pattern composed of three or more layers of cord-like structures of enlarged well-differentiated hepatocytes (Fig. 3*G*). At 10 months, 100% of the caFGFR1 livers exhibited hepatocellular carcinoma compared with only 1 in 7 of WT (Fig. 3*B*). Although

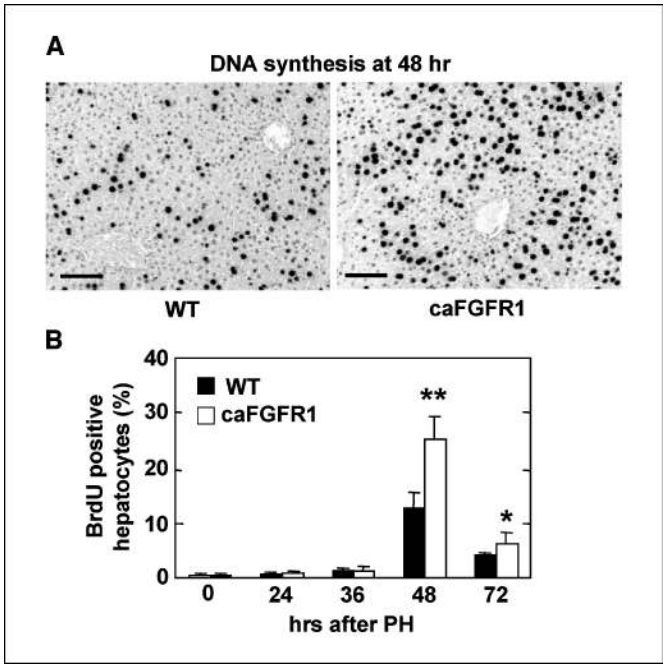


**Figure 2.** Increased incidence of DNA synthesis in regenerating livers expressing ectopic hyperactive FGFR1. *A,* BrdUrd incorporation in WT and transgenic livers 48 hours after surgery. *B,* quantitative analysis of BrdUrd incorporation. *Columns,* mean of 2-month-old mice ($n = 4$ for both WT and caFGFR1 mice) at the indicated times after surgery; *bars,* SD. **, $P < 0.01$; *, $P < 0.05$. Livers were induced to regenerate by partial hepatectomy (see Materials and Methods). Bar, 100 μm.

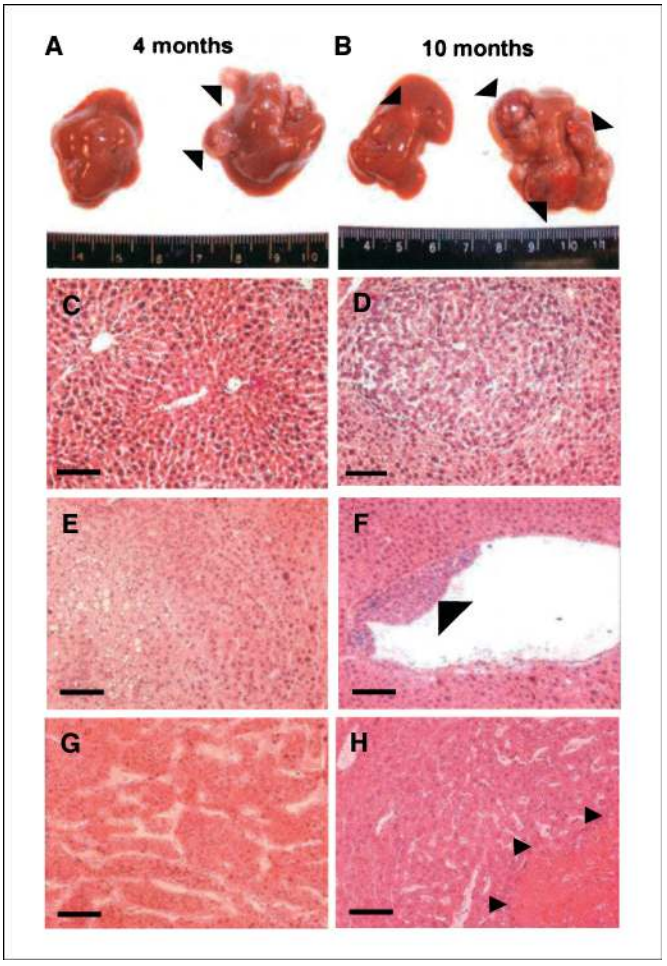


**Figure 3.** Ectopic hyperactive FGFR1 in hepatocytes accelerates incidence of both diethylnitrosamine-induced adenoma and hepatocellular carcinoma. *A* and *B,* livers from WT (*left*) and caFGFR1 transgenic mice (*right*). *Arrowheads,* notable surface hepatomas of different sizes. *C,* normal morphology of diethylnitrosamine-treated WT liver at 4 months. *D,* adenoma at 4 months in a caFGFR1 liver. *E,* fatty liver within an adenoma lesion at 6 months in caFGFR1 liver. *F,* invasive hepatocellular carcinoma lesion in a caFGFR1 liver at 6 months. *Arrowhead,* adherent neoplastic hepatocytes on the luminal side of a large blood vessel. *G,* typical trabecular structure of well-differentiated hepatocellular carcinoma in a caFGFR1 liver at 8 months. *H,* necrosis (*arrowheads*) commonly observed in hepatocellular carcinoma lesions in specifically WT livers at 12 months. Bar, 100 μm.

caFGFR1 accelerated diethylnitrosamine-initiated hepatocarcinogenesis, it had no apparent effect on mortality rate over 12 months of observation.

Tumor burden indicated by the ratio of liver weight to total body weight further confirmed the effect of chronic ectopic hepatocyte FGFR1 in promotion of the diethylnitrosamine-induced hepatocarcinogenesis. During a 12-month period, weight of livers as a percentage of body weight increased at most 5% in 39 diethylnitrosamine-treated WT mice observed, whereas weight of livers increased up to 3-fold in individual caFGFR1 mice (Table 1). Despite a significant increase in incidence of adenomas in the caFGFR1 mice at 4 months, tumor burden was not significant due to the small size of adenomas relative to hepatocellular carcinoma lesions. Tumor burden in the caFGFR1 mice increased significantly with the increase in the development of hepatocellular carcinoma at 8 months in transgenic mice. By 10 months of age, the weight of livers in the transgenic mice was >10% of total body weight, an increase twice that in WT mice. These results indicate that in addition to acceleration of total tumor incidence and development of hepatocellular carcinoma the chronic ectopic activity of FGFR1 underlies a much larger liver tumor burden than that observed in diethylnitrosamine-treated WT mice. At 12 months, tumor-bearing WT livers exhibited areas of intense necrosis expected of tumors of such size (Fig. 3*H*). Such marked necrosis was notably absent from 8- to 10-month-old tumors in caFGFR1 livers of similar size or larger.

**Ectopic hepatocyte FGFR1 accelerates rate of DNA synthesis without effect on apoptosis.** We determined whether hepatocyte FGFR1 promoted hepatomas by acceleration of cell division or reduction in apoptosis in adenoma and hepatocellular carcinoma lesions of similar size in WT and caFGFR1 livers. Consistent with the extremely low mitotic index in normal resting liver (32), only an occasional BrdUrd-positive hepatocyte was observed in both WT and caFGFR1 livers before appearance of tumors (data not shown). Rate of DNA synthesis in adenomas of livers of caFGFR1 mice at 4 to 8 months was about twice that of adenomas of comparable size in WT mice at 6 to 10 months (Fig. 4*A* and *B*). Although the rate of DNA synthesis was about the same between adenoma and hepatocellular carcinoma lesions in WT livers at all times sampled, it was dramatically higher in caFGFR1 hepatocellular carcinoma lesions relative to WT lesions (Fig. 4*A* and *B*). In contrast, no significant difference in rate of apoptosis assessed by the TUNEL assay was observed in the size-paired samples of adenoma and hepatocellular carcinoma from WT and caFGFR1 livers (Fig. 4*C* and *D*). The rate of apoptosis increased progressively from adenoma to hepatocellular carcinoma in both WT and transgenic mice. These results indicate that the acceleration of diethylnitrosamine-induced hepatomas by FGFR1 may be in part to its strong mitogenic activity rather than an increase in cell survival.

**Ectopic caFGFR1 coincident with elevation of the MAPK pathway confers a growth advantage on derived hepatoma cells.** To study the properties of isolated parenchymal hepatocyte-like hepatoma cells, we established cultures of hepatoma cells derived from diethylnitrosamine-induced hepatocellular carcinoma nodules of the same size and stage from both caFGFR1 at 10 months and WT livers at 12 months. Hepatocellular carcinoma from both sources gave rise to continuous cell lines in which >90% of cells sustained a hepatocyte-like morphology typical of differentiated hepatoma cells that dominate hepatocellular carcinoma *in vivo*. Two cell lines established from each type of hepatocellular carcinoma expressed and sustained equal levels of mouse serum albumin mRNA as well as equal levels of endogenous mouse FGFR1 (Fig. 5*A*). Immunochemical analysis with anti-FLAG antiserum against the $NH_2$ terminus of the transgene and an anti-FGFR1 antibody against the COOH terminus (c-FGFR1) indicated that expression of the full-length albumin promoter-driven caFGFR1 was sustained in the cell lines from the caFGFR1 hepatomas (Fig. 5*A*). Analysis of expression of FGF1 and FGF2 by RT-PCR and RPA in the cell lines indicated that they expressed low levels of mRNA (data not shown). Consistent with the presence of

**Table 1.** Hepatic tumors in diethylnitrosamine-treated WT and caFGFR1 mice

| Mouse genotype | Months after birth | Tumor incidence | Hepatocellular carcinoma incidence | Tumor burden (liver weight/body weight × 100) |
|---|---|---|---|---|
| WT | 4 | 0/6 (0) | 0/6 (0) | 5.12 ± 0.18 |
| | 6 | 2/9 (22) | 0/9 (0) | 4.89 ± 0.33 |
| | 8 | 5/9 (56) | 0/9 (0) | 5.75 ± 0.61 |
| | 10 | 5/7 (71) | 1/7 (14) | 6.85 ± 0.59 |
| | 12 | 7/8 (87.5) | 4/8 (50) | 7.86 ± 1.78 |
| caFGFR1 | 4 | 4/9 (44)* | 0/9 (0) | 5.02 ± 0.47 |
| | 6 | 7/10 (70) | 1/10 (10) | 5.48 ± 0.34 |
| | 8 | 7/8 (87.5) | 3/8 (37.5) | 6.93 ± 1.35* |
| | 10 | 8/8 (100) | 8/8 (100)† | 12.6 ± 5.8* |
| | 12 | 5/5 (100) | 5/5 (100)* | 13.5 ± 3.62‡ |

NOTE: A single i.p. injection of 10 μg/g body weight diethylnitrosamine was given to mice at 15 days of age. Incidence/total animals examined was scored as described in Materials and Methods and percentages are indicated in parentheses. Tumor burden was estimated by liver weight divided by total body weight ± SD ($n$ = no. animals indicated under incidence). Significance of difference in the transgenic mice from WT mice at the same time is indicated.

*$P < 0.05$.

†$P < 0.001$.

‡$P < 0.01$.

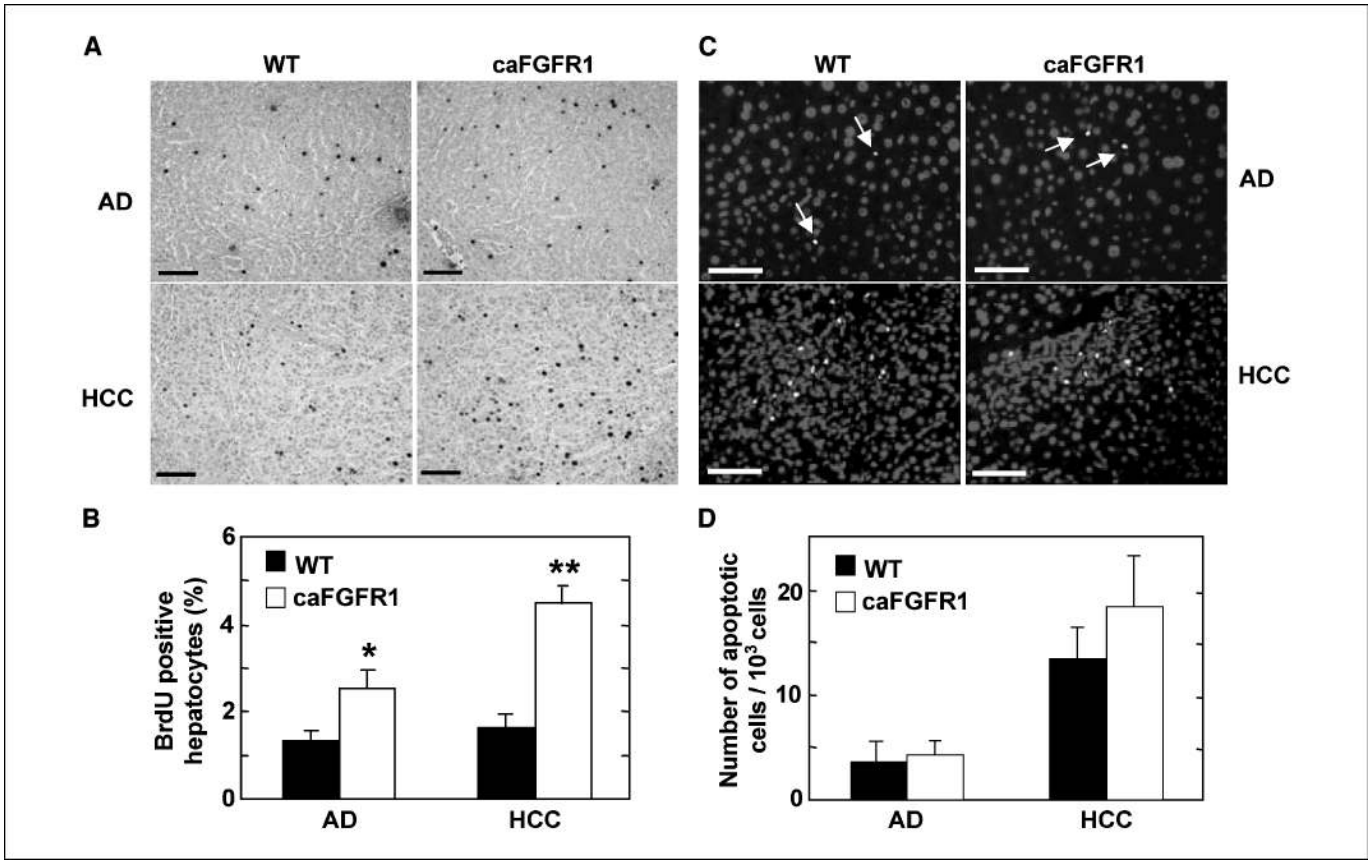


**Figure 4.** Increased DNA synthesis in caFGFR1 livers without a change in rate of apoptosis. *A* and *B,* comparative rates of DNA synthesis in adenoma (*AD*) and hepatocellular carcinoma (*HCC*) of similar sizes in WT and caFGFR1 livers. *C* and *D,* comparative incidence of apoptotic nuclei in adenoma and hepatocellular carcinoma of similar size in WT and caFGFR1 livers. DNA synthesis was measured by BrdUrd incorporation and apoptotic nuclei was measured by the TUNEL assay as described in Materials and Methods. Twelve adenomas from nine WT livers at 6 to 10 months and seven caFGFR1 livers at 4 to 8 months were sampled. Eight hepatocellular carcinomas from five WT mice from 10 to 12 months and seven caFGFR1 mice at 8 to 12 months were analyzed in both proliferation and apoptosis assays. *A* and *C,* representative fields from similar-sized adenomas from WT at 8 months and caFGFR1 at 6 months. Fields shown for hepatocellular carcinoma represent similar-sized WT tumors at 12 months and caFGFR1 tumors at 10 months. *B* and *D,* quantitative data determined by count of cells in two to three fields (×200 for DNA synthesis and ×300 for the TUNEL assay) from the above adenomas and four to five fields from the above hepatocellular carcinoma per tissue section for three different sections. Counts from the three sections per tumor were averaged. *Columns,* mean of average values for different tumors examined; *bars,* SD. *, $P < 0.01$; **, $P < 0.001$. Bar, 100 μm.

caFGFR1, ERK1/2, a common downstream signaling target of activated FGFR1, was constitutively phosphorylated in cultures from the caFGFR1 livers relative to cells from hepatocellular carcinoma from WT livers in serum-free medium (Fig. 5*A*). To determine whether this constitutive activity translated into a growth advantage for the cell population derived from hepatocellular carcinoma from the caFGFR1 livers, growth rates were examined by [$^3$H]thymidine incorporation. At 10% serum, DNA synthesis was similar in cultures derived from hepatocellular carcinoma of both WT and caFGFR1 livers (Fig. 5*B*). However, in serum-free medium, DNA synthesis in cultures derived from hepatocellular carcinoma from caFGFR1 livers exceeded those from WT livers by 2.5-fold (Fig. 5*B*). Addition of FGF2 to the WT hepatoma cells partly relieved their disadvantage in serum-free medium but could not restore DNA synthesis to levels in the presence of serum (Fig. 5*B*). We further compared cell population growth rates at 10% and 0.5% serum. Consistent with DNA synthesis at 10% serum, cell population growth rates were similar in cultures derived from hepatocellular carcinoma from the WT and caFGFR1 livers (Fig. 5*C*). However, cell number in hepatocellular carcinoma cultures at 0.5% serum from the caFGFR1 livers exceeded that from the WT livers by 3-fold after 96 hours of culture (Fig. 5*D*). Taken together, these results suggest that the persistent activity of ectopic FGFR1 in hepatoma cells directly confers a growth advantage to them under deficient environmental conditions.

**Increased expression of endogenous murine FGFR1 and VEGF in diethylnitrosamine-induced hepatomas.** We determined the expression of both human caFGFR1 transgene and endogenous murine FGFR1 (mFGFR1) at the mRNA level in eight paired adenomas and hepatocellular carcinomas of similar size in both caFGFR1 and WT livers. Expression of the human transgene was persistent at all stages throughout the 12-month observation period. This indicated retention of differentiated state of the tumors with respect to expression of the albumin promoter (Fig. 6*A* and *B*). Elevated expression of endogenous murine FGFR1 that is very low in normal resting liver tissue was observed in 63% (5 of 8) of adenomas from WT livers and 100% of those expressing caFGFR1 (Fig. 6*A*). Endogenous FGFR1 was activated in all hepatocellular carcinomas examined (Fig. 6*B*). These data suggested that expression of FGFR1 is elevated early at the adenoma stage of hepatoma development. On average, it was higher in both adenomas and hepatocellular carcinoma of similar size expressing the hyperactive FGFR1 transgene. Ectopic expression of FGFR1

may be a useful marker for staging hepatoma progression in addition to its biological effect on the process.

A hallmark of large hepatocellular carcinomas in the diethylnitrosamine-induced caFGFR1 livers was the absence of severe necrosis relative to tumors of comparable size that appear later in WT livers (Fig. 3*H*). Because necrosis indicates hypoxia and insufficient vascularization that limits size and rate of tumor development, this suggested that hepatocyte FGFR1 may promote development of hepatocellular carcinoma by promotion of neovascularization. FGF2, a potential activating ligand for ectopic FGFR1 in tumor cells and resident FGFR1 in endothelial cells, has been reported to synergize with angiogenic VEGF in promotion of neovascularization (33). Several reports suggest that the angiogenic activity of FGF2 on endothelial cells is indirect and mediated through stimulation of expression of VEGF and its receptors (34, 35). Thus, we examined expression of VEGF at the mRNA level by RPA. Analysis of expression in several normal mouse livers, adenomas, and surrounding normal tissue of eight paired livers in the diethylnitrosamine-induced caFGFR1 and WT livers indicated that VEGF mRNA levels were below the threshold

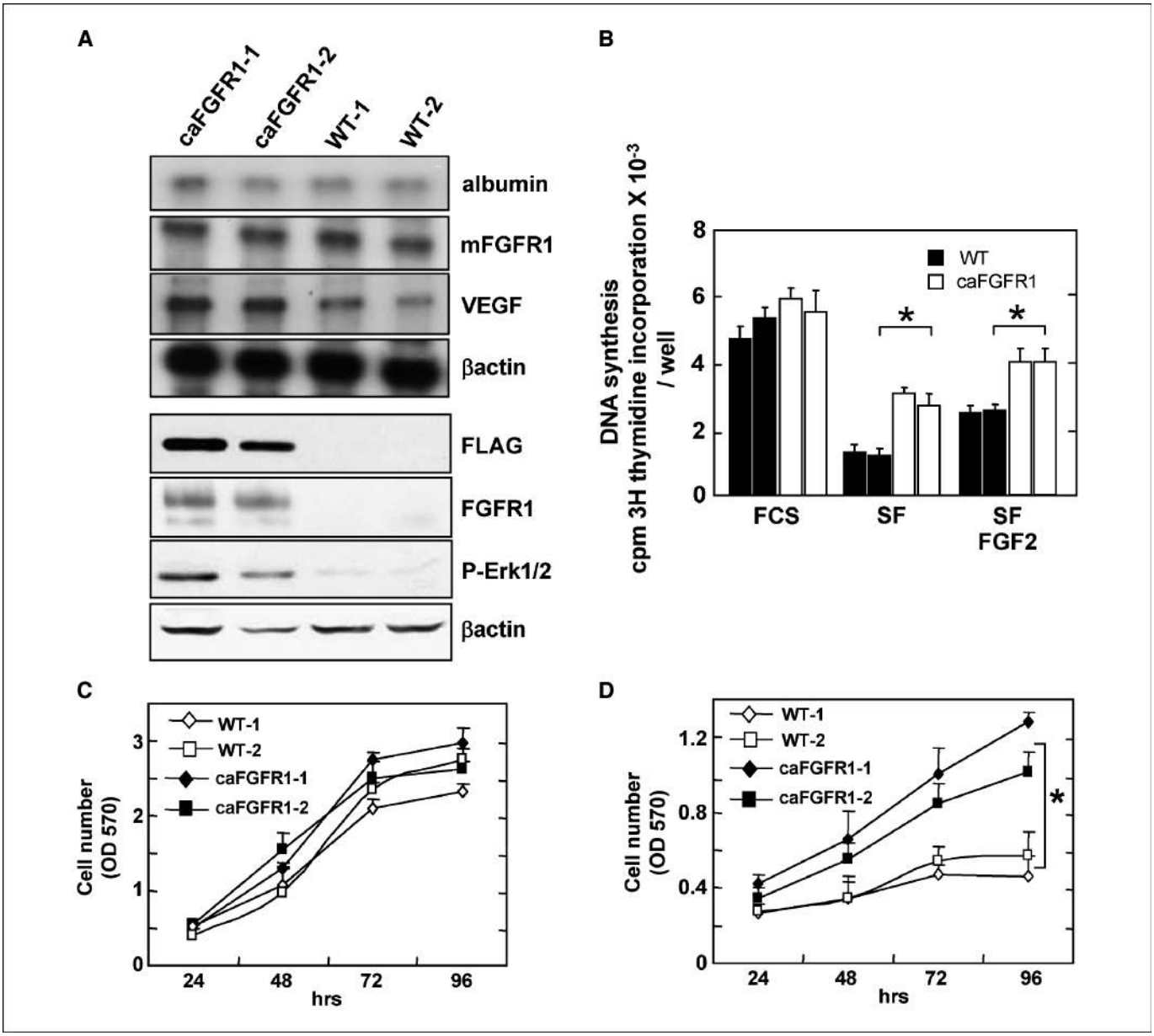


**Figure 5.** Hyperactive FGFR1 confers a growth advantage on hepatocellular carcinoma–derived hepatoma cells. Cell lines were established from hepatocellular carcinoma lesions in WT and caFGFR1 livers as described in the text. Data from two independently established cell lines by methods described in Materials and Methods. *A,* expression of mouse albumin, murine FGFR1, VEGF, full-length caFGFR1, and ERK1/2 activity in WT and caFGFR1 hepatoma cells. Albumin, murine FGFR1, and VEGF were assessed by RPA. Control β-actin was assessed by RPA or Western blot. caFGFR1 was detected with anti-FLAG antibody against the $NH_2$ terminus and an antibody against a human FGFR1 peptide sequence in the COOH terminus. Activated phosphorylated ERK1/2 was detected with antibody specific for phosphorylated ERK1/2. *B,* DNA synthesis. Cells were cultured in 10% FCS or serum-free medium (*SF*) with and without FGF2 (20 ng/mL) for 24 hours before addition of [$^3$H]thymidine. Each column represents an independent cell line. *C* and *D,* cell population growth rates. Increase in cell numbers were assessed in 10% (*C*) and 0.5% (*D*) serum as described in Materials and Methods. *Points,* mean of 12 wells from three independent experiments (cells from different stock cultures) of four wells each per time point for both DNA synthesis and cell growth assays; *bars,* SD. *, $P < 0.001$.

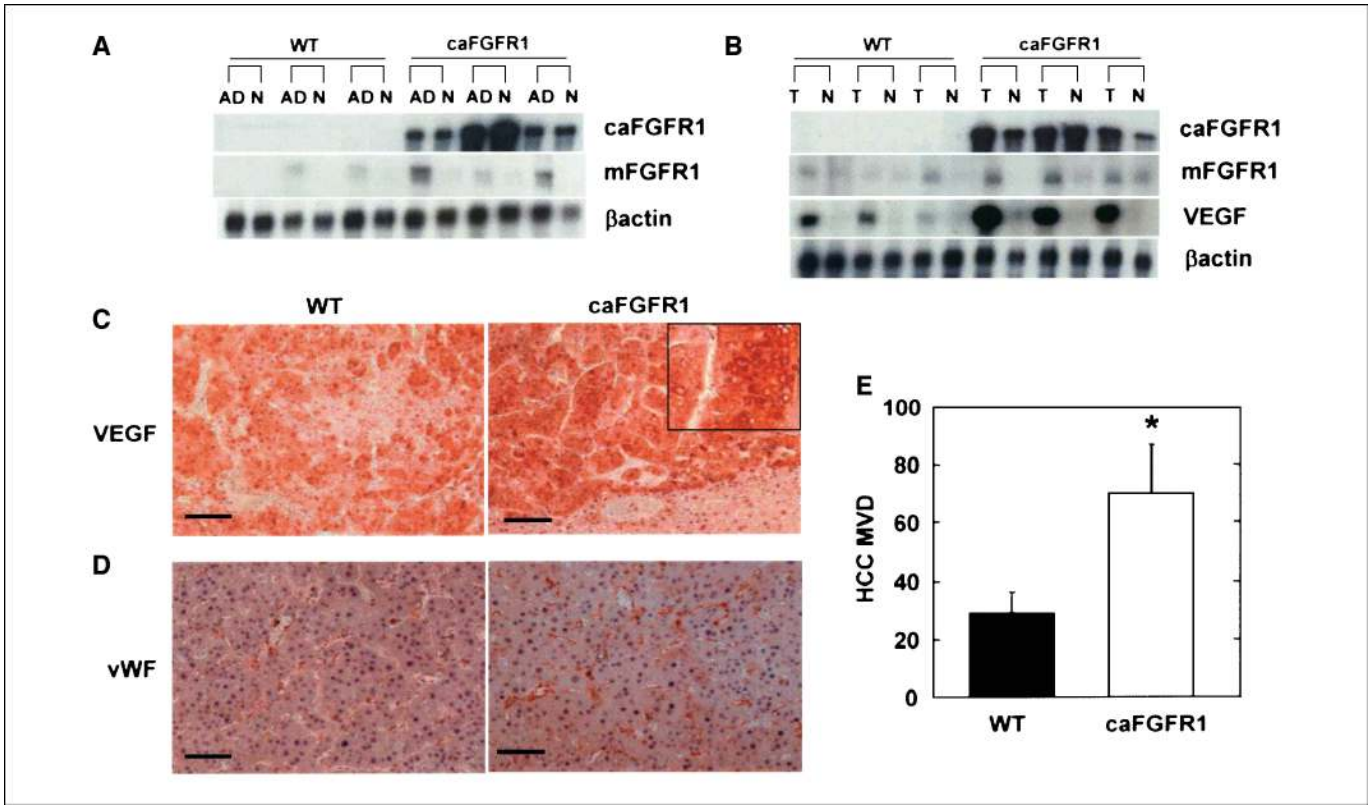


**Figure 6.** Elevated VEGF expression and angiogenesis in specifically hepatocellular carcinoma expressing hyperactive FGFR1. *A* and *B,* expression of the caFGFR1 transgene and endogenous murine FGFR1 in adenomas (*A*) and hepatocellular carcinoma (*B*). *N,* adjacent host liver tissue; *T,* hepatocellular carcinoma; *AD,* adenoma. Representative of the expression pattern in three of eight individual tumors from eight different WT and caFGFR1 host livers analyzed. Adenomas of similar size were derived from WT mouse livers at 6 to 10 months and caFGFR1 livers at 4 to 8 months. Hepatocellular carcinomas of similar size were derived from WT mice at 10 to 12 months and caFGFR1 mice at 8 to 12 months. Autoradiograms of caFGFR1 and mFGFR1 exposed for 24 and 72 hours, respectively. *C,* association of VEGF with hepatoma cells. *D* and *E,* increase in MVD in hepatocellular carcinoma from caFGFR1 livers. Indicated sections in (*D*) are representative of three to four fields examined at ×200 magnification from eight hepatocellular carcinomas from seven different caFGFR1 mice at 8 to 12 months and five WT mice at 10 to 12 months. MVD was quantified as described in Materials and Methods in hepatocellular carcinoma of similar sizes in caFGFR1 and WT livers. *Columns,* mean determined as in Fig. 5; *bars,* SD. *, $P < 0.01$. Bar, 100 μm.

of detection by RPA (data not shown). Expression was detected in hepatocellular carcinoma lesions of WT mouse livers, but the level varied among individuals (Fig. 6*B*). VEGF mRNA levels were invariably higher in caFGFR1 livers although still very low or undetectable in adjacent tissue. The expression of VEGF mRNA in hepatoma cells derived from the transgenic mouse tumors was 3.5 times that observed in WT hepatoma cells (Fig. 5*A*). Immunohistochemical analysis of tissue sections indicated that VEGF was abundant and associated with the hepatoma cells (Fig. 6*C*, *inset*). Immunochemical analysis with anti-vWf further revealed that the mean MVD was significantly higher in hepatocellular carcinoma of comparable size from caFGFR1 mice than those from WT mice (Fig. 6*D*). Quantitative analysis indicated that the MVD in hepatocellular carcinoma from the caFGFR1 mice was 2.7 times that of WT mice ($P < 0.01$; Fig. 6*E*). These data suggest that chronically active ectopic FGFR1 stimulates expression of VEGF in hepatoma cells. The VEGF may act in a paracrine mode to promote neovascularization, reduce necrosis, and thus accelerate rate of development of the diethylnitrosamine-induced tumors.

## Discussion

The aberrant expression of members of the FGF signaling family is commonly observed during progression to malignancy (24, 25). FGFR1, whose expression is normally limited to embryonic progenitors of mature differentiated parenchymal cells or nonparenchymal mesenchymal-derived cells in adult tissues, commonly appears in differentiated tumor cells that emerge from adult tissues (27, 36). In adult resting liver, mature hepatocytes express FGFR4 at high levels, whereas FGFR1, whose expression is overall very low in resting liver, resides in nonparenchymal cells or mature parenchymal cell progenitors (17, 20). Similar to many tumor-derived cells, FGFR1 and activating FGFs for it are ectopically expressed at elevated levels in differentiated hepatoma cells in culture (26, 28). Here, we show by gene targeting to albumin-expressing hepatocytes that in contrast to FGFR4 (21) ectopic FGFR1 in the hepatocyte enhances the regenerative response of hepatocytes to partial hepatectomy. The sustained activity of ectopic FGFR1 in the absence of an activating FGF was achieved by use of a caFGFR1 mutant transgene, caFGFR1. Despite the chronic activity from the time of activation of the albumin promoter, no overt or microscopic cellular or biochemical abnormalities associated with liver neoplasia or preneoplasia was observed throughout the lifetime of the animals. This was quite different from the effect of targeting FGFR1 to mature prostate (29, 37) and mammary secretory epithelial cells (38) where it caused a severe age-dependent progressive glandular hyperplasia characterized by appearance of preneoplastic lesions. We conclude that resting mature hepatocytes are largely immune

to similar effects caused by the presence of persistently hyperactive FGFR1.

Although chronic activity of FGFR1 in the hepatocyte failed to produce liver abnormalities, we show that it is a strong promoter of hepatoma induced by a single perinatal exposure to the hepatocyte-activated procarcinogen diethylnitrosamine. Diethylnitrosamine is thought to induce hepatocellular carcinoma from mature hepatocytes where the caFGFR1 transgene resides (39), which are similar to human hepatocellular carcinoma in several respects relative to other modes of hepatoma induction (40, 41). Lesions characteristic of first adenoma and then hepatocellular carcinoma appeared in the transgenic mouse livers at least 2 and 4 months earlier than their respective appearance in WT mice. The incidence of hepatocellular carcinoma in livers expressing hyperactive FGFR1 was 100% by 10 months compared with an incidence of only 50% at 12 months in WT livers. At 10 months, hyperactive FGFR1 caused a liver tumor burden judged by increase in liver weight over body weight nearly twice that observed in WT livers.

The current study indicates that the chronic activity of ectopic FGFR1 in hepatocytes promotes diethylnitrosamine-initiated hepatocellular carcinoma by at least two mechanisms. Firstly, consistent with the enhanced rate of DNA synthesis in hepatocytes observed during regeneration of normal liver after partial hepatectomy, hyperactive FGFR1 confers a constitutive growth advantage on derived hepatoma cells. This was evident in the 2-fold higher incidence of DNA synthesis within adenomas. It was even more dramatic in the 3-fold increase observed in hepatocellular carcinoma lesions in the transgenic liver tumors compared with WT. Hyperactive FGFR1 caused no apparent decrease in rate of apoptosis, suggesting that the increased rate of tumor growth results from an increased rate of cell division. Hepatoma cells derived from tumors expressing caFGFR1 exhibited a distinct growth advantage in culture relative to tumors derived from WT livers. This correlated with constitutively elevated levels of activated ERK1/2, a marker of the MAPK signaling pathway. The MAPK signaling pathway is the most commonly observed pathway directly linked to FGFR1 activity in diverse cell contexts (42, 43). FGFR1 is the strongest activator of the MAPK pathway among the four FGFR kinase isotypes (44, 45). This suggests that chronic activation of the MAPK pathway by hyperactive FGFR1 is potentially a major driving force for accelerated development and progression of the diethylnitrosamine-induced hepatomas.

In addition to the growth advantage conferred by hyperactive FGFR1 in hepatomas, we show it may also contribute to tumor size by increased angiogenesis mediated by VEGF. Although hepatocellular carcinoma is generally recognized as a hypervascular cancer, necrotic areas were obvious in WT hepatocellular carcinoma tumors at 12 months that were notably less frequent in tumors of similar or even larger size from the transgenic livers. This correlated with a marked increase in vascularization in the transgenic tumors and an average 5-fold increase in VEGF expression that appears to be associated with the hepatoma cells. FGF2 and VEGF are two of the most widely studied endothelial cell mitogens and angiogenesis factors exhibiting powerful activity when applied externally in a wide variety of experimental systems (46). FGF2 is expressed in most hepatoma cells in culture and frequently expressed at elevated levels in hepatoma lesions, although reports vary in how much is in the hepatoma cells and how much is in the neighboring nonparenchymal cells, including endothelial cells (26, 28, 47, 48). Moreover, FGF2 is an activator of FGFR1 in a wide variety of cellular contexts, making it difficult to dissect whether the effect of elevated FGF2 is on hepatoma cells expressing ectopic FGFR1 or resident FGFR1 in endothelial or other nonparenchymal cells (49, 50). Several studies indicate that paracrine VEGF originating from a nonendothelial cell (51) or autocrine VEGF originating in the endothelial cell (34) may mediate the effects of FGF2 on angiogenesis. Our approach bypassed the need for activating FGF2 or a compensating FGF ligand for activation of hepatoma FGFR1. This indicates that activated FGFR1 in hepatoma cells directly causes elevation of VEGF expression that likely originates from the hepatoma cells to enhance angiogenesis.

In summary, we show that although the abnormal activation of normally mesenchymal-derived or embryonic FGFR1 in the hepatocyte and its chronic activity cannot cause neoplasia on its own, it is a powerful promoter of hepatocellular carcinoma development in conjunction with primary initiating carcinogens as diethylnitrosamine that targets the mature hepatocyte. The promotion may occur early in progression by the strong mitogenic activity of FGFR1 in the hepatocyte context and later by hypervascularization mediated by paracrine VEGF required for larger tumors. We used a natural developmental mutant resulting in caFGFR1 to ensure hyperactivity in absence of an activating FGF. To date, no constitutively activating mutations in FGFR1 have been reported associated with tumors in general and hepatomas in particular. A screen for such mutants that are common in several developmental disorders is warranted. Our results suggest that the activity of specifically FGFR1 in the hepatoma cells may be a target for both antiproliferative and antiangiogenic therapies for treatment of hepatomas.

## Acknowledgments

Received 7/11/2005; revised 10/28/2005; accepted 12/1/2005.

**Grant support:** National Institutes of Diabetes, Digestive and Kidney Diseases grant R01DK35310 and National Cancer Institute grants R01CA59971 and U01CA84296.

The costs of publication of this article were defrayed in part by the payment of page charges. This article must therefore be hereby marked *advertisement* in accordance with 18 U.S.C. Section 1734 solely to indicate this fact.

We thank Dr. S. Thorgeirsson for the albumin promoter and Addie Embry for excellent technical assistance.

## References

1. Feitelson MA, Sun B, Satiroglu Tufan NL, Liu J, Pan J, Lian Z. Genetic mechanisms of hepatocarcinogenesis. Oncogene 2002;21:2593–604.
2. Anthony PP. Hepatocellular carcinoma: an overview. Histopathology 2001;39:109–18.
3. Lee GH, Merlino G, Fausto N. Development of liver tumors in transforming growth factor α transgenic mice. Cancer Res 1992;52:5162–70.
4. Factor VM, Kao CY, Santoni-Rugiu E, Woitach JT, Jensen MR, Thorgeirsson SS. Constitutive expression of mature transforming growth factor β1 in the liver accelerates hepatocarcinogenesis in transgenic mice. Cancer Res 1997;57:2089–95.
5. Kanzler S, Meyer E, Lohse AW, et al. Hepatocellular expression of a dominant-negative mutant TGF-β type II receptor accelerates chemically induced hepatocarcinogenesis. Oncogene 2001;20:5015–24.
6. Sakata H, Takayama H, Sharp R, Rubin JS, Merlino G, LaRochelle WJ. Hepatocyte growth factor/scatter factor overexpression induces growth, abnormal development, and tumor formation in transgenic mouse livers. Cell Growth Differ 1996;7:1513–23.
7. Cadoret A, Desbois-Mouthon C, Wendum D, et al. c-myc-induced hepatocarcinogenesis in the absence of IGF-I receptor. Int J Cancer 2005;114:668–72.
8. McKeehan WL, Wang F, Kan M. The heparan sulfate-fibroblast growth factor family: diversity of structure

and function. Prog Nucleic Acid Res Mol Biol 1998;59:135–76.
9. Wang F, McKeehan WL. The fibroblast growth factor (FGF) signaling complex. In: Bradshaw R, Dennis E, editors. Handbook of cell signaling. Vol. I. New York: Elsevier; 2003. p. 265–70.
10. Jung J, Zheng M, Goldfarb M, Zaret KS. Initiation of mammalian liver development from endoderm by fibroblast growth factors. Science 1999;284:1998–2003.
11. Yu C, Wang F, Jin C, et al. Role of fibroblast growth factor type 1 and 2 in carbon tetrachloride-induced hepatic injury and fibrogenesis. Am J Pathol 2003;163:1653–62.
12. Nagasaki T, Lieberman MA. Liver contains heparin-binding growth factors as the major growth factor for cultured fibroblasts. Hepatology 1991;13:6–14.
13. Kan M, Huang JS, Mansson PE, Yasumitsu H, Carr B, McKeehan WL. Heparin-binding growth factor type 1 (acidic fibroblast growth factor): a potential biphasic autocrine and paracrine regulator of hepatocyte regeneration. Proc Natl Acad Sci U S A 1989;86:7432–6.
14. Presta M, Statuto M, Rusnati M, Dell'Era P, Ragnotti G. Characterization of a $M_r$ 25,000 basic fibroblast growth factor form in adult, regenerating, and fetal rat liver. Biochem Biophys Res Commun 1989;164:1182–9.
15. Hioki O, Minemura M, Shimizu Y, et al. Expression and localization of basic fibroblast growth factor (bFGF) in the repair process of rat liver injury. J Hepatol 1996;24:217–24.
16. Steiling H, Muhlbauer M, Bataille F, Scholmerich J, Werner S, Hellerbrand C. Activated hepatic stellate cells express keratinocyte growth factor in chronic liver disease. Am J Pathol 2004;165:1233–41.
17. Hu Z, Evarts RP, Fujio K, Marsden ER, Thorgeirsson SS. Expression of fibroblast growth factor receptors flg and bek during hepatic ontogenesis and regeneration in the rat. Cell Growth Differ 1995;6:1019–25.
18. Steiling H, Wustefeld T, Bugnon P, et al. Fibroblast growth factor receptor signalling is crucial for liver homeostasis and regeneration. Oncogene 2003;22:4380–8.
19. Weinstein M, Xu X, Ohyama K, Deng CX. FGFR-3 and FGFR-4 function cooperatively to direct alveogenesis in the murine lung. Development 1998;125:3615–23.
20. Kan M, Wu X, Wang F, McKeehan WL. Specificity for fibroblast growth factors determined by heparan sulfate in a binary complex with the receptor kinase. J Biol Chem 1999;274:15947–52.
21. Yu C, Wang F, Kan M, et al. Elevated cholesterol metabolism and bile acid synthesis in mice lacking membrane tyrosine kinase receptor FGFR4. J Biol Chem 2000;275:15482–9.
22. Inagaki T, Choi M, Moschetta A, et al. Fibroblast growth factor 15 functions as an enterohepatic signal to regulate bile acid homeostasis. Cell Metab 2005;2:217–25.
23. Yu C, Wang F, Jin C, Wu X, Chan WK, McKeehan WL. Increased carbon tetrachloride-induced liver injury and fibrosis in FGFR4-deficient mice. Am J Pathol 2002;161:2003–10.
24. Klint P, Claesson-Welsh L. Signal transduction by fibroblast growth factor receptors. Front Biosci 1999;4:D165–77.
25. Powers CJ, McLeskey SW, Wellstein A. Fibroblast growth factors, their receptors and signaling. Endocr Relat Cancer 2000;7:165–97.
26. Kin M, Sata M, Ueno T. Basic fibroblast growth factor regulates proliferation and motility of human hepatoma cells by an autocrine mechanism. J Hepatol 1997;27:677–87.
27. Hu Z, Evarts RP, Fujio K, et al. Expression of transforming growth factor α/epidermal growth factor receptor, hepatocyte growth factor/c-met and acidic fibroblast growth factor/fibroblast growth factor receptors during hepatocarcinogenesis. Carcinogenesis 1996;17:931–8.
28. Ogasawara S, Yano H, Iemura A, Hisaka T, Kojiro M. Expressions of basic fibroblast growth factor and its receptors and their relationship to proliferation of human hepatocellular carcinoma cell lines. Hepatology 1996;24:198–205.
29. Wang F, McKeehan K, Yu C, Ittmann M, McKeehan WL. Chronic activity of ectopic type 1 fibroblast growth factor receptor tyrosine kinase in prostate epithelium results in hyperplasia accompanied by intraepithelial neoplasia. Prostate 2004;58:1–12.
30. Pinkert CA, Ornitz DM, Brinster RL, Palmiter RD. An albumin enhancer located 10 kb upstream functions along with its promoter to direct efficient, liver-specific expression in transgenic mice. Genes Dev 1987;1:268–76.
31. Yu C, Wang F, Jin C, Huang X, McKeehan WL. Independent repression of bile acid synthesis and activation of c-Jun N-terminal kinase (JNK) by activated hepatocyte fibroblast growth factor receptor 4 (FGFR4) and bile acids. J Biol Chem 2005;280:11707–14.
32. Taub R. Liver regeneration: from myth to mechanism. Nat Rev Mol Cell Biol 2004;5:836–47.
33. Yoshiji H, Kuriyama S, Yoshii J. Synergistic effect of basic fibroblast growth factor and vascular endothelial growth factor in murine hepatocellular carcinoma. Hepatology 2002;35:834–42.
34. Seghezzi G, Patel S, Ren CJ, et al. Fibroblast growth factor-2 (FGF-2) induces vascular endothelial growth factor (VEGF) expression in the endothelial cells of forming capillaries: an autocrine mechanism contributing to angiogenesis. J Cell Biol 1998;141:1659–73.
35. Majima M, Hayashi I, Muramatsu M, Katada J, Yamashina S, Katori M. Cyclo-oxygenase-2 enhances basic fibroblast growth factor-induced angiogenesis through induction of vascular endothelial growth factor in rat sponge implants. Br J Pharmacol 2000;130:641–69.
36. Yan G, Fukabori Y, McBride G, Nikolaropolous S, McKeeha WL. Exon switching and activation of stromal and embryonic fibroblast growth factor (FGF)-FGF receptor genes in prostate epithelial cells accompany stromal independence and malignancy. Mol Cell Biol 1993;13:4513–22.
37. Freeman KW, Welm BE, Gangula RD, et al. Inducible prostate intraepithelial neoplasia with reversible hyperplasia in conditional FGFR1-expressing mice. Cancer Res 2003;63:8256–63.
38. Welm BE, Freeman KW, Chen M, Contreras A, Spencer DM, Rosen JM. Inducible dimerization of FGFR1: development of a mouse model to analyze progressive transformation of the mammary gland. J Cell Biol 2002;157:703–14.
39. Sell S. Heterogeneity and plasticity of hepatocyte lineage cells. Hepatology 2001;33:738–50.
40. Graveel CR, Jatkoe T, Madore SJ, Holt AL, Farnham PJ. Expression profiling and identification of novel genes in hepatocellular carcinomas. Oncogene 2001;20:2704–12.
41. Lee JS, Chu IS, Mikaelyan A, et al. Application of comparative functional genomics to identify best-fit mouse models to study human cancer. Nat Genet 2004;36:1306–11.
42. Campbell JS, Wenderoth MP, Hauschka SD, Krebs EG. Differential activation of mitogen-activated protein kinase in response to basic fibroblast growth factor in skeletal muscle cells. Proc Natl Acad Sci U S A 1995;92:870–4.
43. Chikazu D, Hakeda Y, Ogata N. Fibroblast growth factor (FGF)-2 directly stimulates mature osteoclast function through activation of FGF receptor 1 and p42/p44 MAP kinase. J Biol Chem 2000;275:31444–50.
44. Shaoul E, Reich-Slotky R, Berman B, Ron D. Fibroblast growth factor receptors display both common and distinct signaling pathways. Oncogene 1995;10:1553–61.
45. Hart KC, Robertson SC, Kanemitsu MY, Meyer AN, Tynan JA, Donoghue DJ. Transformation and Stat activation by derivatives of FGFR1, FGFR3, and FGFR4. Oncogene 2000;19:3309–20.
46. Cross MJ, Claesson-Welsh L. FGF and VEGF function in angiogenesis: signalling pathways, biological responses and therapeutic inhibition. Trends Pharmacol Sci 2001;22:201–7.
47. Motoo Y, Sawabu N, Nakanuma Y. Expression of epidermal growth factor and fibroblast growth factor in human hepatocellular carcinoma: an immunohistochemical study. Liver 1991;11:272–7.
48. Chow NH, Cheng KS, Lin PW, et al. Expression of fibroblast growth factor-1 and fibroblast growth factor-2 in normal liver and hepatocellular carcinoma. Dig Dis Sci 1998;43:2261–6.
49. Tanghetti E, Ria R, Dell'Era P, et al. Biological activity of substrate-bound basic fibroblast growth factor (FGF2): recruitment of FGF receptor-1 in endothelial cell adhesion contacts. Oncogene 2002;21:3889–97.
50. Sahni A, Francis CW. Stimulation of endothelial cell proliferation by FGF-2 in the presence of fibrinogen requires $\alpha_v\beta_3$. Blood 2004;104:3635–41.
51. Goto F, Goto K, Weindel K, Folkman J. Synergistic effects of vascular endothelial growth factor and basic fibroblast growth factor on the proliferation and cord formation of bovine capillary endothelial cells within collagen gels. Lab Invest 1993;69:508–17.